Scanning Electrochemical Microscopy. 34. Potential Dependence of the Electron-Transfer Rate and Film Formation at the Liquid/Liquid Interface

Michael Tsionsky and Allen J. Bard*

Department of Chemistry and Biochemistry, The University of Texas at Austin, Austin, Texas 78712

Michael V. Mirkin*

Department of Chemistry and Biochemistry, Queens College−CUNY, Flushing, New York 11367

Received: May 3, 1996; In Final Form: September 4, 1996[⊗]

The potential drop across the interface between two immiscible electrolyte solutions (ITIES), $\Delta_w^o \varphi$, can be quantitatively controlled and varied by changing the ratio of concentrations of the potential-determining ion in the two liquid phases. This approach was used to study the potential dependence of the rate constant for electron transfer (ET) at the ITIES (k_f) by scanning electrochemical microscopy (SECM) with no external potential bias applied. The Tafel plot obtained for ET between aqueous $Ru(CN)_6^{4-}$ and the oxidized form of zinc porphyrin in benzene was linear with a transfer coefficient, $\alpha = 0.5$, determined from the slope of a plot of ln k_f vs $\Delta_w^o \varphi$, in agreement with conventional ET theory. The observed change in the ET rate with the interfacial potential drop cannot be attributed to concentration effects and represents the potential dependence of the apparent rate constant. This result is discussed in relation to the interface thickness and structure. The SECM was also used to study solid phase formation at the interface at high concentrations of supporting electrolyte (tetrahexylammonium perchlorate, $THAClO_4$) in benzene. The precipitation of the THA^+ and $Ru(CN)_6^{4-}$ compound occurred when its solubility product was exceeded. This process leads to the formation of a thin three-dimensional interfacial layer, which can be unambiguously distinguished from monolayer adsorption. The approach curve analysis yields the composition of such a layer. Its thickness can also be probed.

Introduction

Interest in heterogeneous electron-transfer (ET) reactions motivates the search for experimental systems suitable for testing available theories. Heterogeneous rate constants ($k°$, cm/s) have been measured for numerous electrochemical reactions involving dissolved species, adsorbed moieties, immobilized enzymes, and redox centers bound to self-assembled monolayers and confined to redox polymer films. Unfortunately, experimental data obtained for these systems are often complicated by surface and solvent effects and experimental artifacts.[1] For example, heterogeneous ET reactions at metallic electrodes are often too fast for conventional electrochemical measurements,[2] so that many $k°$ values measured earlier by transient measurements at millimeter-sized electrodes were distorted by resistive potential drop and double-layer charging. Steady-state measurements employing micrometer-sized electrodes are apparently free from this problem and yield $k°$ values much higher than those obtained with larger electrodes.[3,4] However, these values are still orders of magnitude lower than ones predicted by Marcus theory. By using a compact organic monolayer as a spacer between redox centers and a metal substrate, one can slow down the ET rate, study its potential dependence over a wide range of potentials, and thus measure the reorganization energy, λ.[2] Nevertheless, questions remain about the effect of monolayer orientation, defects, the local environment of the bound redox centers, and the influence of the nature of the spacers on the ET rate.[5] The redox processes in redox polymers are probably even more complex, and the extraction of the ET parameters from experimental data is by no means straightforward.[6] Thus, the interface between two immiscible electrolyte solutions (ITIES) seems to be a more tractable experimental system for heterogeneous ET studies.

The ET between redox species confined to two immiscible solvents was first demonstrated by Guainazzi et al. in 1975,[7] and different theoretical treatments for this process have been proposed over the last several years.[8−12] Severe experimental problems complicate extraction of the kinetic parameter values from conventional electrochemical measurements at the ITIES (e.g., by cyclic voltammetry). These include the difficulty of discrimination between rate limitation by ET and by ion transfer (IT), distortions from the double-layer charging current, *iR*-drop in the highly resistive nonaqueous solvents, and the limited potential window for studying ET in the absence of currents controlled by IT.[13] Because of these difficulties, experimental studies of ET at the ITIES are scarce. Schiffrin et al. used cyclic voltammetry to study interfacial ET.[14a,b] The Nicholson method[15] was employed to extract $k°$ values from cyclic voltammograms, thus implicitly assuming that the potential dependence of the rate constant obeys the Butler−Volmer equation. This assumption could be checked by fitting the whole cyclic voltammogram to the theory, but this was not reported. The use of the Butler−Volmer model (as well as the Marcus model) is justified only if most of the interfacial potential drop occurs between the reacting redox moieties across the ITIES. This assumption has not yet been corroborated by experiments. Moreover, if the redox reaction occurs within a mixed solvent layer[13a,c] or if the reacting species can partially penetrate the phase boundary,[9b,c] the picture of a potential-driven heterogeneous ET becomes ambiguous. Accordingly, Samec et al.[16] found that the rate constant for ET between ferrocene in nitrobenzene and aqueous ferricyanide was almost potential-independent. Girault[13c] pointed out that the apparent potential dependence of the ET rate may

[⊗] Abstract published in *Advance ACS Abstracts,* November 1, 1996.

S0022-3654(96)01270-1 CCC: $12.00

be attributed to the change in concentrations of the reactants near the interface rather than to activation control.

Some of these questions can be clarified by studying the potential dependence of the ET rate. To our knowledge, the only reported study of the potential dependence of the ET rate at the ITIES employed impedance measurements,[17] where the authors assumed that the conventional theory of faradaic impedance and the Butler−Volmer equation were directly applicable to the ITIES. However, in this paper the measured transfer coefficient was found to be potential-dependent; that is, the experimental results did not agree with the Butler−Volmer model. The authors attributed this discrepancy to unspecified double-layer effects and ionic adsorption.

As discussed in an earlier paper,[18] the use of SECM eliminates many of the above mentioned experimental problems. In a typical SECM/ITIES experiment, a tip ultramicroelectrode (UME) with a radius a is placed in an upper liquid phase containing the reduced form of the redox species, R_1. When the tip is held at a positive potential, R_1 reacts at the tip surface to produce the oxidized form of the species, O_1. When the tip approaches the ITIES, the mediator can be regenerated at the interface via the bimolecular redox reaction between O_1 in the aqueous phase (w) and R_2 in the organic phase (o),

$$O_1(w) + R_2(o) \xrightarrow{\kappa_{12}} R_1(w) + O_2(o) \qquad (1)$$

and the tip current, i_T, increases with a decrease in the tip−ITIES separation, d (i.e., shows positive feedback). The kinetics of such a reaction can be evaluated from the tip current−distance (or approach) curve. If no regeneration of R_1 occurs, the ITIES blocks mediator diffusion to the tip, so i_T decreases at smaller d; that is, negative feedback is observed. While conventional studies of the ITIES have been carried out at externally biased polarizable ITIES, in SECM measurements, a nonpolarizable ITIES is poised by the concentrations of the potential-determining ions, providing a constant driving force for the ET process. In this way, ET can be quantitatively separated from the IT processes, allowing one unambiguously to distinguish between concentration effects and a true potential dependence of the rate constant.

Another problem of interest is two- or three-dimensional phase formation at the ITIES. Adsorption of surfactants at the boundary between two liquids has been the subject of numerous investigations.[13] Electrodeposition of metals[19] and conductive polymers[20] at the liquid/liquid interface was also demonstrated. Film formation at the ITIES was observed with an aqueous solution containing K^+ and an organic phase with ClO_4^-,[21] where the relatively low solubility of the compound formed in both phases, $KClO_4$, caused its precipitation at the interface. The film formed at the ITIES, like the interface itself, is not easily accessible by either optical or electrochemical measurements.[22] One can approach such a film with the SECM tip and obtain information about its nature, composition, and thickness. In a previous SECM study,[18] all reactants and products of the interfacial reaction were soluble, none of them reacted with the supporting electrolyte to form an insoluble product, and their adsorption was assumed to be negligible. ET rate measurements were reported in this earlier SECM study, but these were somewhat compromised by the small solubility of the tip-generated species in the aqueous phase. Here we study a system where this is less of a problem and also try to distinguish between reactant adsorption and formation of a thicker layer and assess the effect of such a layer on the ET process.

Experimental Section

Chemicals. $NaClO_4$, NaCl, and $Na_4Fe(CN)_6$ from Johnson Matthey (Ward Hill, MA), ferrocene (Fc) and zinc 5,10,15,20-tetraphenyl-21*H*,23*H*-porphine (ZnPor) from Aldrich (Milwaukee, WI), and benzene and bromobenzene from J. T. Baker (Phillisburg, NJ) were used as received. Tetrahexylammonium perchlorate ($THAClO_4$, Fluka Chemika, Switzerland) was recrystallized twice from an ethyl acetate/ether (9:1) mixture and was dried under vacuum overnight at room temperature. $Na_4Ru(CN)_6$ was synthesized from $RuCl_3$ (Aldrich) by the method used for $K_4Ru(CN)_6$,[23] but with NaOH and NaCN instead of potassium hydroxide and cyanide. $Na_4Ru(CN)_6$ was recrystallized five times from methanol/water and was dried under vacuum at 50 °C overnight. All aqueous solutions were prepared from deionized water (Milli-Q, Millipore Corp.).

Electrodes and Electrochemical Cells. Pt wires (25-, 10-, and 5-μm diameter) (Goodfellow, Cambridge, U.K.) were heat-sealed in glass capillaries, and then SECM tips were prepared as described previously.[24] The tip electrode was polished before each measurement. A three-electrode configuration was used, and all electrodes were always placed in the top phase. A Ag/AgCl electrode in saturated KCl was used as the reference electrode. A NaCl and $NaClO_4$ solution was used as an ionic bridge between the reference electrode and organic phase. A 2-mL glass vial mounted on a vibration-free stage served as the cell for SECM experiments. To measure the heterogeneous rate constant between $ZnPor^+$ and $Ru(CN)_6^{4-}$, the top phase (volume, ~0.5 mL) contained a 0.25 M $THAClO_4$ and 0.5 mM ZnPor benzene solution, and the bottom phase (volume, 1.0 mL) contained a 0.1 M NaCl, 0.01−2 M $NaClO_4$, and 1−100 mM $Na_4Ru(CN)_6$ aqueous solution. To measure the surface excess of $Ru(CN)_6^{4-}$ on the ITIES, a 0.1 M NaCl, 0.01 M $NaClO_4$, and 10−100 mM $Na_4Ru(CN)_6$ aqueous solution was used as the top phase and a 0−1 M $THAClO_4$ bromobenzene solution was used as the bottom phase. Perchlorate was the only ion common to both phases for all experiments. The transfer of this ion between the two phases maintained electroneutrality by compensating for the positive charge injected into the water by the ET reaction. The ratio of bulk concentrations of ClO_4^- in aqueous and organic phase, $[ClO_4^-]_w/[ClO_4^-]_o$, determined the potential drop across the ITIES. Among all of the ionic species contained in our system (i.e., Na^+, Cl^-, $Ru(CN)_6^{3/4-}$, THA^+, $ZnPor^{0/+}$, and ClO_4^-), only ClO_4^- and electrons could readily cross the interface.

SECM Apparatus and Procedure. The basic apparatus used for the SECM experiments has been described previously.[25] Before the SECM measurements, the tip electrode was positioned in the top phase and was biased at a potential where the tip process was diffusion-controlled. The approach curves were obtained by moving the tip toward the ITIES and recording i_T as a function of d. The data were acquired using software written by D. O. Wipf. The coordinate of the ITIES ($d = 0$) was determined from the sharp increase (or decrease, if the bottom phase contained no redox species) in tip current that occurred when the tip touched the ITIES.

Results and Discussion

Potential Drop across the ITIES. The relative values of the potential drop across the ITIES were obtained from cyclic voltammograms of either ZnPor or Fc at a 12.5-μm-radius microdisk electrode in benzene solution. The reversible half-wave potential of either couple was measured with respect to the Ag/AgCl electrode connected to the benzene solution by an ionic bridge. The junction potential between saturated KCl and an aqueous solution of NaCl and $NaClO_4$ was assumed not to depend strongly on the $NaClO_4$ concentration. The cell used

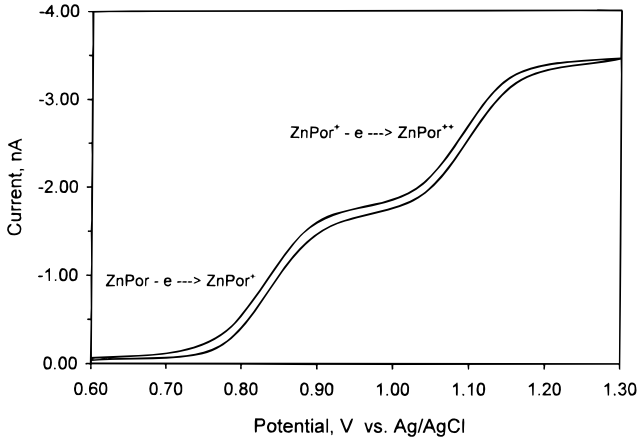

Figure 1. Steady-state voltammogram of ZnPor in benzene at a 25-μm-diameter Pt microdisk UME. Solution contained 1 mM ZnPor and 0.25 M $THAClO_4$. Sweep rate was 25 mV/s.

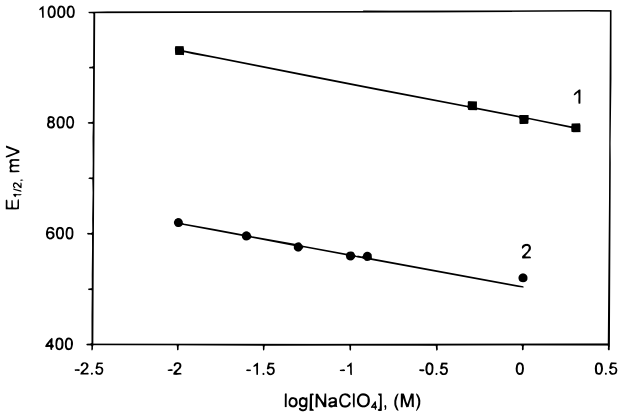

Figure 2. Dependence of half-wave potentials of Fc (curve 1) and ZnPor (curve 2) oxidations in benzene on ClO_4^- concentration in aqueous phase. Half-wave potentials were extracted from steady-state voltammograms obtained at a 25-μm-diameter Pt UME. Benzene contained 0.25 M $THAClO_4$ and either 5 mM Fc or 1 mM ZnPor. All potentials were measured with respect to Ag/AgCl reference in aqueous phase. See text for cell description.

to measure the interfacial potential drop can be represented as follows:

$$\text{Ag/AgCl/H}_2\text{O, KCl (sat'd)/H}_2\text{O, 0.1 M NaCl, 0.01}-\text{2 M NaClO}_4\text{//benzene, 0.25 M THAClO}_4\text{, 1 mM ZnPor (or 5 mM Fc)/Pt} \quad (2)$$

The Galvani potential difference ($\Delta_w^o \varphi$) at the liquid junction (//) should be governed by the ratio of ClO_4^- concentration in water and the organic phase:[13]

$$\Delta_w^o \varphi = \Delta_w^o \varphi^o_{ClO_4^-} - 0.059 \log \frac{[ClO_4^-]_w}{[ClO_4^-]_o} \quad (3)$$

$[ClO_4^-]_o$ was maintained constant and equal to 0.25 M in all our experiments. Thus, $\Delta_w^o \varphi$ should be a linear function of $[ClO_4^-]_w$ with a slope of -59 mV per decade. Accordingly, the half-wave potential of any electrochemical reaction in benzene, measured with respect to the aqueous reference electrode, should shift by 59 mV to more negative values with a decade increase in $[ClO_4^-]_w$.

A typical steady-state voltammogram of ZnPor obtained at a 25-μm tip in the above cell (Figure 1) consists of two well-defined waves corresponding to two one-electron oxidations of ZnPor to $ZnPor^+$ and then to $ZnPor^{2+}$. Curve 1 in Figure 2 represents the dependence of half-wave potential of the first

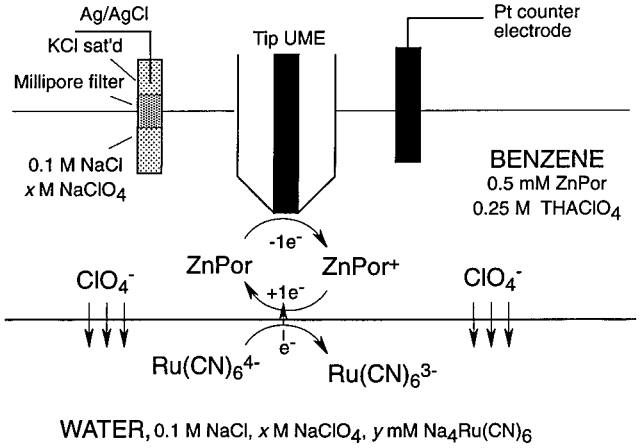

Figure 3. Schematic diagram of the application of SECM in the feedback mode measurement of the kinetics of ET between $ZnPor^+$ in benzene and $Ru(CN)_6^{4-}$ in water. Electroneutrality was maintained by transfer of perchlorate ions across the interface.

oxidation of ZnPor in benzene on $[ClO_4^-]_w$. This essentially linear dependence shows an approximately 140-mV change in $\Delta_w^o \varphi$ with an increase of $[ClO_4^-]_w$ from 0.01 to 2 M. The slope of this straight line, 61 ± 2 mV per decade, agrees well with theory. A similar slope, 57 ± 3 mV per decade, was found for Fc oxidation (curve 2 in Figure 2). Clearly, the shift in the half-wave potential due to the change of $[ClO_4^-]_w$ should be the same for any redox reaction in the organic phase. The small difference between the two slope values is probably due to the uncertainty in the experimentally found $E_{1/2}$ values. Thus we use the average of the above two values and express the potential drop across the ITIES as

$$\Delta_w^o \varphi = \text{const} - 0.06 \log[ClO_4^-]_w \quad (4)$$

Since the current at the UME in these experiments was on the order of 1 nA, the measured half-wave potentials were essentially unaffected by the *iR*-drop.

Heterogeneous Rate Constant of ET at the ITIES. The scheme of the SECM measurement of the rate of the electron transfer between $ZnPor^+$ in benzene and aqueous $Ru(CN)_6^{4-}$ is presented in Figure 3. The tip electrode generates $ZnPor^+$ ions by oxidation of ZnPor. $ZnPor^+$ diffuses to the ITIES, where it is reduced back to ZnPor by reaction with $Ru(CN)_6^{4-}$:

$$\text{ZnPor} - \text{e} \rightarrow \text{ZnPor}^+ \quad \text{(tip)} \quad (5a)$$

$$\text{ZnPor}^+ + \text{Ru(CN)}_6^{4-} \rightarrow \text{ZnPor} + \text{Ru(CN)}_6^{3-} \quad \text{(ITIES)} \quad (5b)$$

The rate of the mediator regeneration via reaction 5b can be evaluated from the tip current. When no oxidizible species was present in the aqueous phase, the i_T vs d dependence followed the SECM theory for an insulating substrate (curve 5 in Figure 4A). Similar current−distance curves were obtained earlier at the water/nitrobenzene interface.[18] In the presence of $Ru(CN)_6^{4-}$, the tip current increased with a decrease in d; at higher $[Ru(CN)_6^{4-}]$, the i_T vs d curve approached the diffusion limit given by curve 1 in Figure 4A. Reaction 5b injects positive charge into the aqueous phase that is compensated by IT of ClO_4^- from benzene to water. At low concentrations of the common ion (e.g., less than 10 mM),[18] the IT may become the rate-determining step. To avoid this complication, the concentration of ClO_4^- in benzene was kept high (0.25 M) in all ET kinetic experiments.

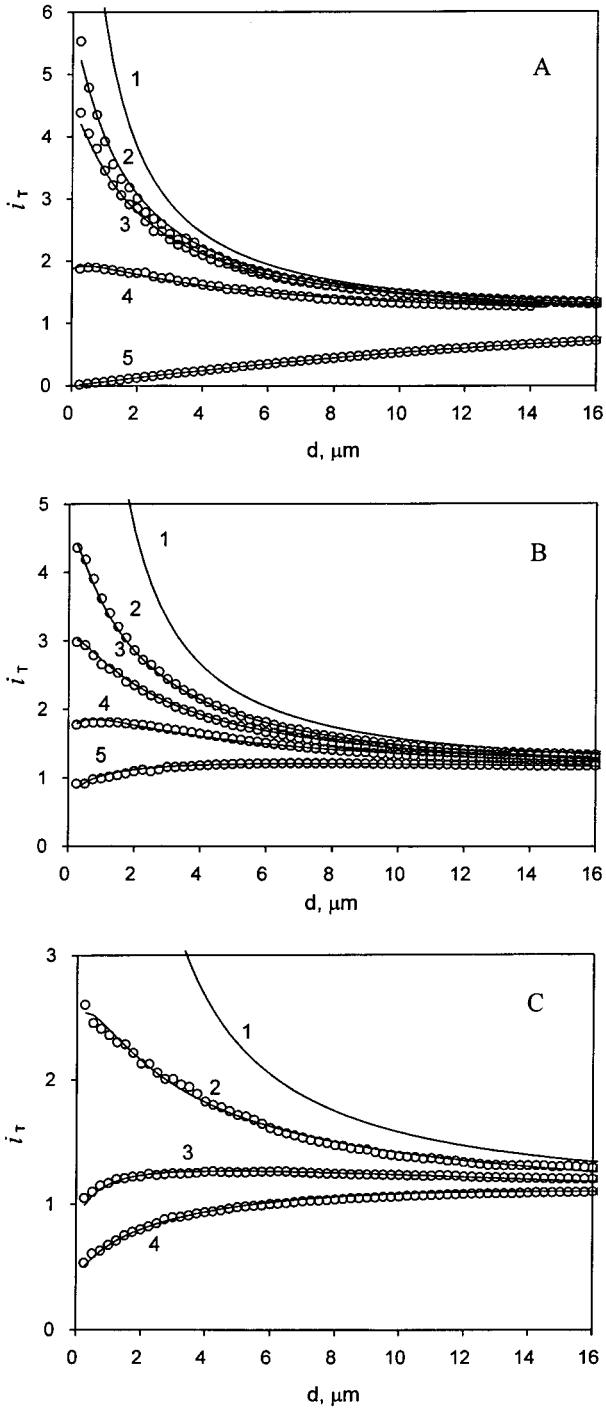

Figure 4. SECM current−distance curves for a 12.5-μm-radius Pt tip UME in benzene solution approaching the water/benzene interface. Benzene was 0.5 mM in ZnPor and 0.25 M in $THAClO_4$. Curve 1 in A, B, and C is the theoretical curve for a diffusion-controlled process obtained using eq 7. The tip potential was held at 0.95 V vs Ag/AgCl, corresponding to the plateau current of first oxidation of ZnPor (Figure 1). The tip was scanned at 0.5 μm/s. The aqueous solution contained (A) 0.1 M NaCl, 0.01 M $NaClO_4$, and (2) 50, (3) 5, (4) 0.5, or (5) 0 mM $Na_4Ru(CN)_6$; (B) 0.1 M NaCl, 0.1 M $NaClO_4$, and (2) 20, (3) 6, (4) 4, or (5) 0.5 mM $Na_4Ru(CN)_6$; (C) 0.1 M NaCl, 1.0 M $NaClO_4$, and (2) 75, (3) 10, or (4) 5 mM $Na_4Ru(CN)_6$; (○) experimental points; (—) theoretical fit obtained from eqs 6a and 6b. See Figure 5 for rate constant values.

When IT is not rate limiting, the following equations can be used to extract the first-order effective heterogeneous ET rate constant from the i_T -d curves:[18]

$$I_T^{\,k} = I_S^{\,k}(1 - I_T^{\,ins}/I_T^{\,c}) + I_T^{\,ins} \quad (6a)$$

$$I_S^{\,k} = 0.78377/L(1 + 1/\Lambda) + [0.68 + 0.3315 \times \exp(-1.0672/L)]/[1 + F(L,\Lambda)] \quad (6b)$$

where I_T^c, I_T^k, and I_T^{ins} represent the normalized tip currents for diffusion-controlled regeneration of a redox mediator, finite substrate kinetics, and insulating substrate (i.e., no mediator regeneration), respectively, at a normalized tip−substrate separation, $L = d/a$. I_S^k is the kinetically controlled substrate current; $\Lambda = k_f d/D_R$, where k_f is the apparent heterogeneous rate constant (cm/s), and D_R is the diffusion coefficient of the reduced mediator in the top phase; and $F(L,\Lambda) = (11 + 7.3\Lambda)/[\Lambda(110 - 40L)]$. These currents are normalized by the tip current at an infinite tip−substrate separation, $i_{T,\infty} = 4nFaD_Rc_R$. The analytical approximations for I_T^c and I_T^{ins} are

$$I_T^{\,c} = 0.78377/L + 0.3315 \exp(-1.0672/L) + 0.68 \quad (7)$$

$$I_T^{\,ins} = 1/(0.15 + 1.5358/L + 0.58 \exp(-1.14/L) + 0.0908 \exp[(L - 6.3)/(1.017L)]) \quad (8)$$

Equations 6a and 6b were used to fit the families of approach curves obtained at different concentrations of $Ru(CN)_6^{4-}$ and $NaClO_4$ in the water phase (Figure 4). Good agreement between theory (solid line) and experimental data (symbols) was achieved using only one adjustable parameter, Λ. We found k_f values within the range 0.002−0.03 cm/s from the measured Λ values and a diffusion coefficient of ZnPor in benzene of 4.0×10^{-6} cm^2/s obtained by steady-state voltammetry. Dependencies of k_f vs $[Ru(CN)_6^{4-}]$ at different concentrations of $NaClO_4$ in water are shown in Figure 5A. At lower concentrations of $Ru(CN)_6^{4-}$, k_f was proportional to $[Ru(CN)_6^{4-}]$ for any given value of $[ClO_4^-]_w$. The linear concentration dependence of heterogeneous rate constant corresponds to reaction 5b, which is first order with respect to $Ru(CN)_6^{4-}$.

At a given concentration of $Ru(CN)_6^{4-}$, the apparent rate constant depends on the potential drop across the ITIES, which increases with a decrease in the $NaClO_4$ concentration. From Figure 2, one can see that a decrease in $[ClO_4^-]_w$ makes the water phase more negative with respect to the organic phase, thus increasing the driving force for reaction 5b. The dependence of k_f on the concentration of redox species in the bottom phase and driving force can be written as follows:[9b,18]

$$k_f = \text{const}[Ru(CN)_6^{4-}] \exp(-\Delta G^{\ddagger}/RT) \quad (9)$$

where $\Delta G^{\ddagger}$ is the free energy barrier (J/mol). For lower overvoltages, a Butler−Volmer-type approximation can be used

$$\Delta G^{\ddagger} = -\alpha F(\Delta E^{\circ} + \Delta_w^o \varphi) \quad (10)$$

where ΔE° is the difference between standard potentials of two redox couples, F is the Faraday constant, α is the transfer coefficient, and $\Delta_w^o \varphi$ is the potential drop across the ITIES. For two given redox couples (e.g., $Ru(CN)_6^{4-}$ and ZnPor), the ΔE° value is fixed and combination of eqs 10 and 4 yields

$$k_f = \text{const}[Ru(CN)_6^{4-}] \exp(-0.06\alpha \log[ClO_4^-]_w/f) \quad (11a)$$

or

$$\log(k_f) = \text{const'} + \log[Ru(CN)_6^{4-}] - 0.06\alpha \log[ClO_4^-]_w/f \quad (11b)$$

where $f = RT/F$. Thus, the $\log(k_f)$ vs $\log[ClO_4^-]$ dependence for different concentrations of $Ru(CN)_6^{4-}$ should be linear with a slope proportional to α. In agreement with eq 11b, plots of

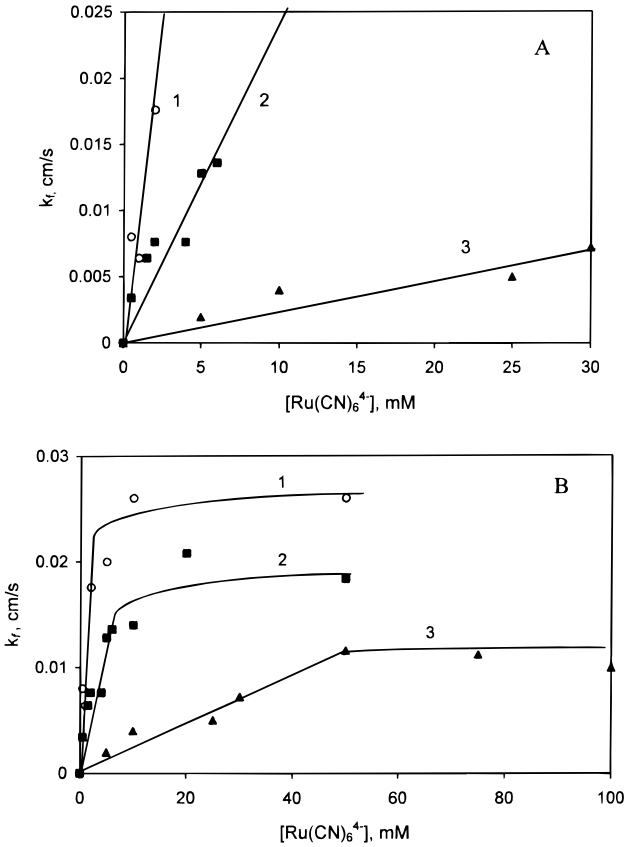

Figure 5. Dependence of the effective heterogeneous rate constant on $[Ru(CN)_6^{4-}]$ at different concentrations of $NaClO_4$ in water. $[ClO_4^-]_w$ = (1) 0.01, (2) 0.1, and (3) 1.0 M. (A) Linear concentration dependencies of k_f obtained at low concentrations of $Ru(CN)_6^{4-}$. The k_f values were used to fit the approach curves in Figure 4 with a = 12.5-μm-diameter and $D_{ZnPor^+} = 4.0 \times 10^{-6}$ cm^2/s. (B) Concentration dependence of k_f levels off at higher $[Ru(CN)_6^{4-}]$.

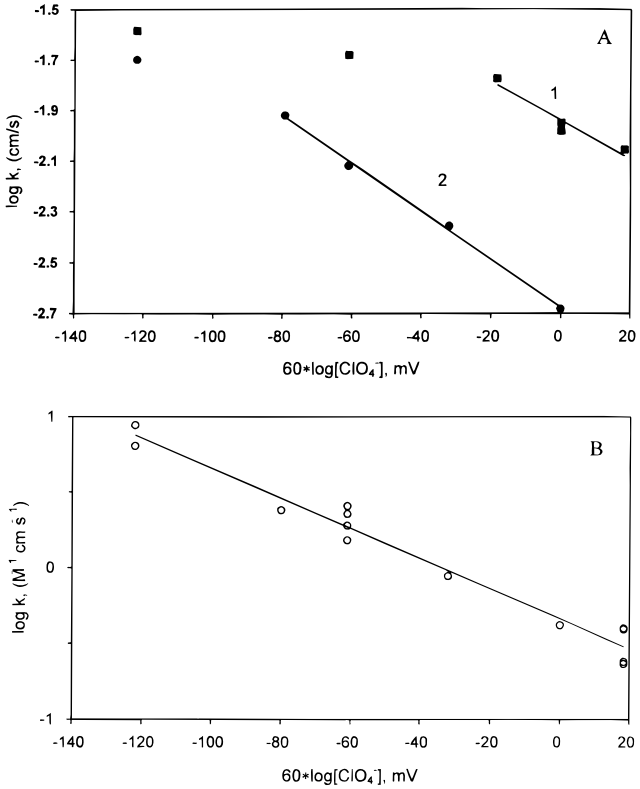

Figure 6. Dependence of the effective heterogeneous rate constant on potential drop across the ITIES at (1) 50 and (2) 5 mM concentrations of $Ru(CN)_6^{4-}$. For other parameters see Figure 4. $\Delta_w^o \varphi$ is expressed in terms of $\log[ClO_4^-]_w$ according to eq 4. (A) At higher $[ClO_4^-]_w$, the linear portions of Tafel plots yield the α values given in the text. Tafel plots deviate from linearity as k_f approaches the diffusion limit. (B) Potential dependence of an effective bimolecular rate constant, $k = k_f/[Ru(CN)_6^{4-}]$ (M^{-1} cm s^{-1}).

$\log(k_f)$ vs $\log[ClO_4^-]_w$ at different concentrations of $Ru(CN)_6^{4-}$ were linear (Figure 6) at higher $[ClO_4^-]_w$, corresponding to less positive $\Delta_w^o \varphi$. At lower $[ClO_4^-]_w$, corresponding to a more positive $\Delta_w^o \varphi$, the ET rate approached the diffusion limit and the $\log(k_f)$ vs $\log[ClO_4^-]_w$ curves tended to level off. This effect is more significant at higher concentrations of $Ru(CN)_6^{4-}$ (curve 1 in Figure 6), for which the k_f values (at the same $\Delta_w^o \varphi$) are higher. Two similar transfer coefficient values were found from the linear portions of the Tafel plots, i.e., $\alpha = 0.49 \pm 0.1$ for 50 mM $Ru(CN)_6^{4-}$ and $\alpha = 0.56 \pm 0.05$ for 5 mM $Ru(CN)_6^{4-}$. Moreover, one can use the data obtained at different concentrations of $Ru(CN)_6^{4-}$ to calculate the effective bimolecular rate constant, $k = k_f/[Ru(CN)_6^{4-}]$ (M^{-1} cm s^{-1}). The data in Figure 6B, taken over a several week period and with different tip electrodes, demonstrate the high reproducibility of the results.

The linear Tafel plots and α values close to 0.5 indicate that conventional ET theory, e.g., for the metal/electrolyte interface, is applicable to heterogeneous reactions at the ITIES. The observed potential dependence of the ET rate cannot be attributed to concentration effects. The rate of the redox reaction increased as the potential of the water side of the ITIES was made more negative and the organic phase became more positive. However, such changes would result in a small decrease in the concentrations of both reactants (i.e., anionic $Ru(CN)_6^{4-}$ in water and cationic $ZnPor^+$ in benzene) at the interface.

Our findings also suggest that the reactants do not significantly penetrate the interfacial boundary. Clearly, the potential dependence of the ET rate is related to the potential drop that exists between the two reacting molecules. If the ET reaction occurred within a fairly thick mixed solvent layer rather than across the thin interfacial boundary, this potential drop would be negligible or at least much smaller than the total $\Delta_w^o \varphi$ value. This would have resulted in $\alpha \ll 0.5$. Thus a thin-boundary model,[9a] rather than a model assuming a significant penetration of species into a mixed solvent layer,[9b,c] is applicable to the ET at the interface between two very low miscibility solvents, like water and benzene. This does not exclude the possibility of the existence of a thin ion-free layer at the interface.[26] Such a layer, separating participants of the redox reaction, would result in a smaller ET rate constant rather than affect the α value.

The above analysis does not include double-layer effects. The possibility of such effects and the applicability of a Frumkin correction have been discussed previously.[13] A quantitative treatment of this problem is difficult because of insufficient information about the interfacial structure. Nevertheless, Katano et al.[12c] considered two situations, i.e., a diffuse layer rate-determining process and an inner layer rate-determining process. In the first case, the theory predicts highly nonlinear Tafel curves. The inner layer effects should result in an apparent transfer coefficient value significantly lower than 0.5. Our experimental data do not confirm either of these predictions, and there is no evidence of a strong double-layer effect on the measured kinetic parameters.

Interfacial Film Formation at the ITIES. At higher concentrations of $Ru(CN)_6^{4-}$ the dependence of k_f vs $[Ru(CN)_6^{4-}]$ levels off (Figure 5b) and the shape of current−distance curves becomes essentially independent of $[Ru(CN)_6^{4-}]$. This behavior is expected when the ET reaction is rapid and mediator diffusion in the gap between the tip and the ITIES becomes rate limiting. This is indeed the case for curve 1 in Figure 5B, where the

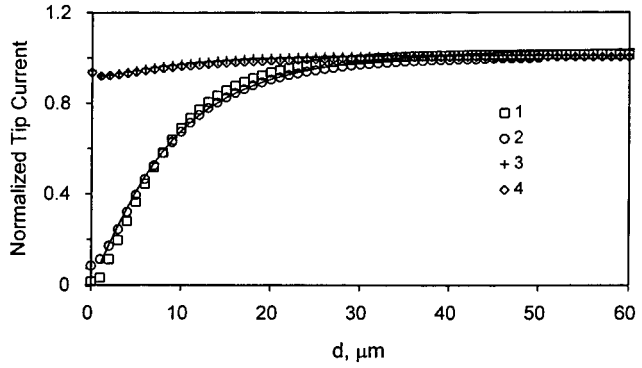

Figure 7. Current−distance curves for a 25-μm-diameter Pt tip UME approaching the bromobenzene/water interface. The tip was in the aqueous solution containing 0.01 M $NaClO_4$, 0.1 M NaCl, and 30 mM $Na_4Ru(CN)_6$. [$THAClO_4$] = (1) 0, (2) 0.01, (3) 0.1, and (4) 0.25 mM. Organic phase contained no redox mediator. Solid line represents SECM theory for an insulating substrate (eq 8). Tip scan rate was 10 μm/s.

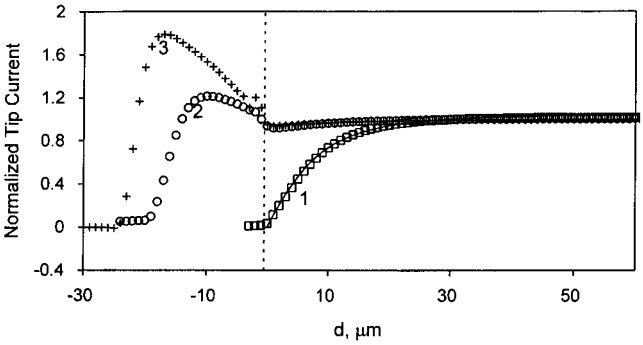

Figure 8. Current−distance curves obtained with different concentrations of $Na_4Ru(CN)_6$ in water and a constant concentration of $THAClO_4$ in bromobenzene. Bromobenzene contained 0.25 M $THAClO_4$. [$Ru(CN)_6^{4-}$] = (1) 10, (2) 30, and (3) 50 mM. Aqueous solution also contained 0.01 M $NaClO_4$ and 1 M NaCl. Solid line represents SECM theory for an insulating substrate (eq 8). Negative distances correspond to the trapping of a water layer inside the organic phase.

limiting value of $k_f = 0.027$ cm/s is close to the upper limit of rate constant accessible under our experimental conditions. The corresponding current−distance curve (curve 2 in Figure 4A) is not very different from the theoretical curve 1 representing the diffusion limit. However, the limiting k_f values in curve 2 and especially in curve 3 (Figure 5B) are much lower and cannot be attributed to diffusion limitations. One should also notice that the increase in the limiting k_f with decreasing $[ClO_4^-]_w$ suggests that the overall process is kinetically controlled.

The independence of the ET rate on [$Ru(CN)_6^{4-}$] points to the existence of the limiting concentration of this species at the interface independent of its bulk concentration. Such saturation can be attributed to either adsorption of $Ru(CN)_6^{4-}$ moieties at the ITIES or formation of some low-solubility compound at the interface. The adsorbed species could be ion pairs formed from the hydrophobic THA^+ and the hydrophilic $Ru(CN)_6^{4-}$.

The SECM was previously used to probe adsorption/desorption phenomena and surface diffusion of electroactive species at solid/liquid interfaces.[27] The UME tip was used to induce desorption of the redox species by depleting its concentration near the substrate via electrolysis. The desorption rate in ref 27 was evaluated from the tip current transients. However, when both desorption and surface diffusion processes are rapid, one should be able to detect adsorbed species from the analysis of steady-state current−distance curves.

To probe any surface excess of $Ru(CN)_6^{4-}$ at the ITIES, we obtained two families of i_T-d curves with no redox species present in the organic phase (Figures 7 and 8). In these experiments, we replaced benzene with the heavier bromobenzene so that the water phase was on top. The i_T-d curves in Figure 7 were obtained with different concentrations of $THAClO_4$ in the organic phase and a constant [$Ru(CN)_6^{4-}$] = 30 mM. Both the reference and the counter electrodes were in the aqueous phase. In this experiment, one would expect the ITIES to behave as a perfect insulator, if there was no accumulation of $Ru(CN)_6^{4-}$ at the interface.[18] Pure negative feedback was indeed observed for all concentrations of [$Ru(CN)_6^{4-}$] when the bromobenzene did not contain $THAClO_4$ (curve 1 in Figure 7). As the concentration of $THAClO_4$ increased, the ITIES behavior remained insulating (curve 2) until [$THAClO_4$] reached some critical value that depended on [$Ru(CN)_6^{4-}$]; for example, the critical value of [$THAClO_4$] was about 60 mM at [$Ru(CN)_6^{4-}$] = 30 mM. After [$THAClO_4$] reached this value, the tip current increased markedly (curve 3) and did not change any further at higher concentrations of $THAClO_4$ (curve 4). The higher values of tip current point to either regeneration of the $Ru(CN)_6^{4-}$ species at the interface (which could not occur because no redox species was present in bromobenzene) or accumulation of $Ru(CN)_6^{4-}$ at the interface. As the $Ru(CN)_6^{4-}$ species is depleted by electrolysis at the tip, desorption (or dissolution) occurs at the interface and results in an i_T significantly higher than expected for pure negative feedback. This phenomenon is very similar to the SECM-induced dissolution of crystals.[28] After the tip penetrated the interface ($d \leq 0$ in Figure 8), the current increased to values higher than the tip current in the bulk; that is, the concentration and diffusion coefficient of $Ru(CN)_6^{4-}$-containing species within the interfacial film are higher than in the bulk aqueous solution.

The family of i_T-d curves obtained at different concentrations of $Ru(CN)_6^{4-}$ in the aqueous phase and constant [$THAClO_4$] (Figure 8) show a very similar effect. For a [$Ru(CN)_6^{4-}$] below the critical value, e.g., about 20 mM at [$THAClO_4$] = 0.25 M, as in Figure 8, insulating behavior was observed (curve 1). When [$Ru(CN)_6^{4-}$] reached this critical value, the tip current increased (curve 2), and a further increase in concentration did not significantly affect the shape of i_T-d curves (curve 3). The reactive behavior of the ITIES at higher [$Ru(CN)_6^{4-}$] cannot be caused by redox active impurities in the organic phase, since this effect would be most noticeable at low concentrations of mediator in the upper phase.[18]

The shape of the portion of the i_T-d curve before the tip touches the ITIES ($d > 0$) is exactly the same for any concentration of $THAClO_4$ and $Ru(CN)_6^{4-}$ below the film formation threshold (Figures 7 and 8). This indicates that the interfacial film forms abruptly when both [$THAClO_4$] and [$Ru(CN)_6^{4-}$] become sufficiently high and the concentration of $Ru(CN)_6^{4-}$-containing species in the film is always the same. This picture is inconsistent with the assumption of an adsorption process at the interface, since the surface excess of the adsorbate would increase gradually with [$Ru(CN)_6^{4-}$] until a saturation value is reached. The sharp transition from reactive to inactive behavior suggests the formation of an insoluble compound between THA^+ and $Ru(CN)_6^{4-}$ at the ITIES when its solubility product is exceeded.

One can determine the composition of the $(THA^+)_n$-$(Ru(CN)_6^{4-})_m$ complex from the values of ion concentrations at which the shape of i_T-d curves changes sharply. Figure 9 shows two concentration regions of $THAClO_4$ and $Ru(CN)_6^{4-}$ corresponding to reactive and inactive SECM responses. Pure negative feedback (open squares below the straight line separating two regions) was observed when no surface accumulation of $Ru(CN)_6^{4-}$ was detectable. Above the straight line (filled squares), interfacial film formation occurs, resulting in a significantly higher tip current. The line between the two regions of Figure 9 can be described by the equation

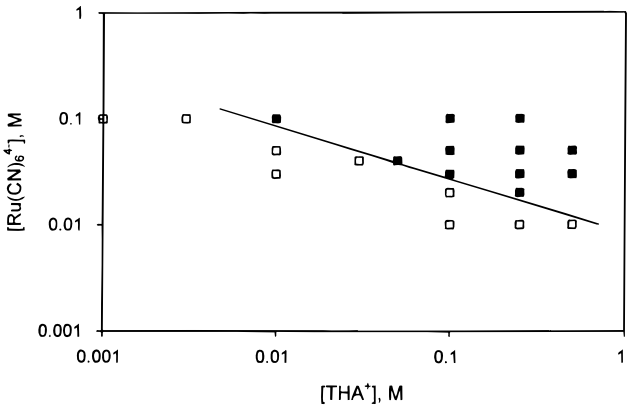

Figure 9. Concentration zone diagram illustrating film formation at the ITIES. The open squares below the straight line correspond to negative feedback current (no film formed); the filled squares above the line correspond to positive feedback due to the film formation. The solid line between the two zones represents the solubility product $[THA^+][Ru(CN)_6^{4-}]^2 = 6 \times 10^{-5}$ M^3.

$[THA^+][Ru(CN)_6^{4-}]^2 = 6 \times 10^{-5}$ M^3. This value may be considered as a solubility product of a precipitate that contains two $Ru(CN)_6^{4-}$ species per one THA^+ and additional cations (e.g., Na^+). When this value is exceeded, a film formed at the ITIES maintains a constant surface concentration of $Ru(CN)_6^{4-}$ moieties. Consequently, k_f becomes independent of the bulk concentration of $Ru(CN)_6^{4-}$. Additional experiments are required to elucidate the rather complex nature of the interfacial film.

The type of film formed at the ITIES depends on the solubility of each component of the film. When the organic phase contained tetrabutylammonium perchlorate ($TBAClO_4$), which is much more soluble in water than $THAClO_4$, a thick film of a TBA^+ and $Ru(CN)_6^{4-}$ compound, visible to the naked eye, was formed in several seconds. In contrast, when the organic phase contained THA^+, the ITIES remained clear and transparent for at least 48 h. From the approach curves in Figure 8, one can see that the distance between the point where the tip touches the ITIES (this corresponds to the sharp increase in i_T) and the point where it leaves the film (where i_T drops near to zero) was always about 20 μm. Although it is tempting to attribute this to film thickness, we believe that the invisible film cannot be this thick. The 20-μm distance reflects trapping of a thin layer of water between the Pt microelectrode and bromobenzene, as previously found in SECM studies.[18] A gradual increase in i_T after the tip touches the interface apparently corresponds to squeezing of this layer. Eventually, the advancing tip contacts the organic phase, and i_T drops to near zero. The almost constant 20-μm distance observed in different experiments is probably due to the use of the same 12.5-μm-radius Pt tip. More spatially resolved information about the film may be obtained using much smaller (nanometer-sized) tips that are less prone to solution trapping.[18]

Another argument in favor of a very thin film comes from the observed potential dependence of the ET rate. Although the interfacial film formation causes deviations from linearity in Tafel plots, the effective rate constant remains strongly potential-dependent. As discussed above, this suggests that the $Ru(CN)_6^{4-}$-containing species in the film and $ZnPor^+$ in benzene are still separated by a thin interfacial boundary and most of the potential drop develops across this boundary.

The interfacial film is well-separated from the aqueous phase, and the water/film boundary is sharp on a submicrometer scale, as shown in Figure 10, where the current increase caused by the tip touching the film occurs over the distance between two nearest points of the approach curve, i.e., 100 nm. The actual

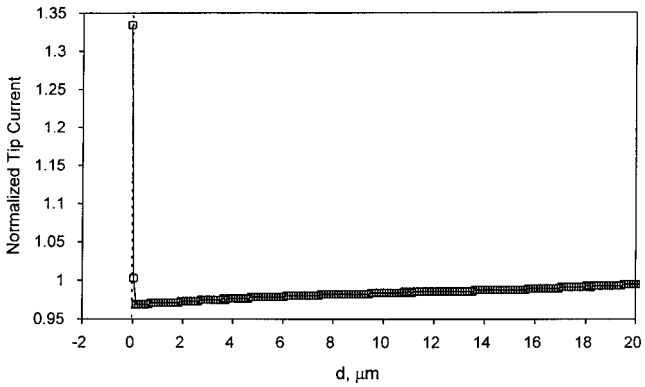

Figure 10. Effect of a 25-μm-diameter Pt tip touching an electroactive film formed by THA^+ and $Ru(CN)_6^{4-}$ at the water/bromobenzene interface. Bromobenzene contained 0.25 M $THAClO_4$. Aqueous solution contained 30 mM $Ru(CN)_6^{4-}$, 0.01 M $NaClO_4$, and 0.1 M NaCl. Concentrations of $Ru(CN)_6^{4-}$ and THA^+ correspond to film formation on the ITIES (see Figure 8). The tip was scanned at 1 μm/s.

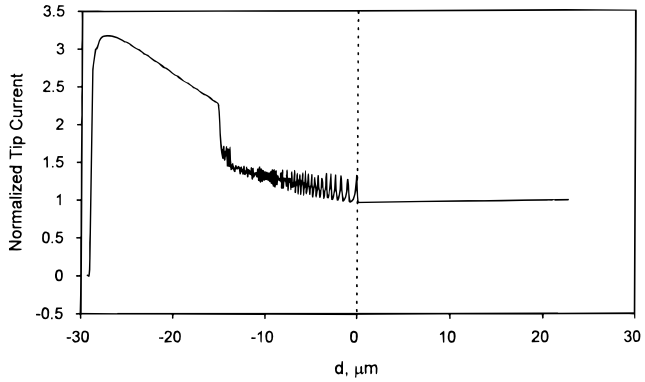

Figure 11. Current oscillations seen as the tip penetrated a water/bromobenzene interface. Experimental conditions are the same as for Figure 10.

thickness of the transition region may be significantly smaller because of resolution limitations and the roughness of a Pt microdisk.

A significant contribution of film dissolution to the tip current suggests that lateral diffusion of electroactive species at the ITIES is rapid. The surface diffusion coefficient should be of the same order of magnitude as the bulk diffusion coefficient for $Ru(CN)_6^{4-}$. This is consistent with high values of surface diffusion coefficients measured recently for different water/hydrocarbon interfaces.[29] The surface diffusion at the solid/liquid interface is usually slower.[27]

Tip current oscillations were often observed after the tip contacted the film (Figure 11). In contrast, no significant noise was observed in similar experiments with no film formed at the ITIES. This high-amplitude periodic noise in i_T might be caused by oscillatory dissolution that was previously observed for different metals and other crystalline materials, e.g., in SECM experiments.[28b] However, the oscillatory dissolution would have produced tip current oscillations before the tip touched the ITIES. Thus we assume that the noisy tip current is due to trapping of a water layer. Apparently, this layer is initially unstable, and its thickness changes periodically. As the advancing tip moves the trapped layer inside the organic phase and squeezes it, the oscillations disappear. This effect was reproducible; one could scan the tip back and forth (e.g., between $d = 0$ and -15 μm in Figure 11) or withdraw it from the bromobenzene into the water phase and approach the ITIES again and record very similar oscillating $i_T - d$ curves.

Approach curves very similar to those in Figures 7 and 8 were obtained when $Fe(CN)_6^{4-}$ was used instead of $Ru(CN)_6^{4-}$.

Although both $Fe(CN)_6^{3/4-}$ and tetraalkylammonium salts have been used frequently in electrochemical studies of the ITIES,[14b,30] film formation effects have not been reported previously, probably because the concentrations used were below the solubility line in Figure 9.

Conclusions

We have used the SECM to investigate ET occurring at the ITIES via a bimolecular reaction between redox species confined to different solvents. The potential drop at the ITIES was poised by the concentrations of the potential-determining ions (ClO_4^-) in both phases, providing a controllable driving force for the ET reaction. Since no external voltage was applied across the ITIES, the described measurements were free of the uncompensated *iR*-drop and charging current problems typical for conventional techniques. Linear dependencies of $\log(k_f)$ on interfacial potential drop (Tafel plots) were measured for the ET between $Ru(CN)_6^{4-}$ in water and ZnPor in benzene with α values close to 0.5. This indicates that conventional ET theories are applicable to the liquid/liquid interface. The observed changes in the ET rate with the interfacial potential drop cannot be attributed to concentration effects and thus represent an actual potential dependence of the apparent rate constant.

The measured α value of 0.5 suggests that the participants of the ET reaction are separated by a thin interfacial boundary rather than a mixed, fairly thick, interfacial layer. Otherwise, the potential drop between two redox molecules would be much smaller than the total $\Delta_w^o \varphi$, and α would be much smaller than 0.5. This does not exclude the possibility of a thin ion-free layer at the interface separating participants of the redox reaction. Such a layer would result in the smaller ET rate constant, but would not affect the α value.

The formation of a thin layer of salt at the ITIES was observed at higher reactant concentrations. The film was a product of interaction of the hydrophobic cation (e.g., THA^+) and the hydrophilic anion (e.g., $Ru(CN)_6^{4-}$) to form a product at the interface that was insoluble in both water and organic solvent. This film formation occurs abruptly when the product of the cation and anion concentrations exceeds the solubility product. This phenomenon can be distinguished from interfacial adsorption that increases gradually with increasing bulk concentration of adsorbing species. The constant concentration of redox moieties within the interfacial film results in a leveling off the k_f vs $[Ru(CN)_6^{4-}]$ dependence (Figure 5B). Probing the thickness and physicochemical properties of interfacial films by SECM with a much smaller (nanometer-sized) probe may be possible.

Acknowledgment. The support of this research by grants from the Robert A. Welch Foundation (A.J.B.) and the National Science Foundation (CHE-9508525, A.J.B.) is gratefully acknowledged. Acknowledgment is made to the Donors of the Petroleum Research Fund administered by the American Chemical Society, for the partial support of this research (M.V.M.). M.V.M. also acknowledges a grant from PSC-CUNY.

References and Notes

(1) Weaver, M. J. *Chem. Rev.* **1992**, *92*, 463. Weaver, M. J. In *Electrified Interfaces in Physics, Chemistry and Biology*; Guidelli, R., Ed.; Kluwer Academic Publishers: The Netherlands, 1992; p 427.

(2) Miller, C. J. In *Physical Electrochemistry: Principles, Methods, and Applications*; Rubinstein, I., Ed.; Marcel Dekker: New York, 1995; p 27.

(3) Bond, A. M.; Oldham, K. B.; Zoski, C. G. *Anal. Chim. Acta* **1989**, *216*, 177.

(4) Montenegro, M. I. In *Research in Chemical Kinetics*, Compton, R. G., Hancock, G., Eds.; Elsevier Science B. V: Amsterdam, 1994; Vol. 2, p 1.

(5) Finklea, H. O. In *Electroanalytical Chemistry*; Bard, A. J., Ed.; Marcel Dekker: New York; Vol. 19, in press.

(6) Zhang, H.; Murray, R. W. *J. Am. Chem. Soc.* **1993**, *115*, 2335.

(7) Guainazzi, M.; Silvestry, G.; Survalle, G. *J. Chem. Soc., Chem. Commun.* **1975**, 200.

(8) (a) Kharkats, Yu. I.; Volkov, A. G. *J. Electroanal. Chem.* **1985**, *184*, 435. (b) Kharkats, Yu. I.; Ulstrup, J. *J. Electroanal. Chem.* **1991**, *308*, 17.

(9) (a) Marcus, R. A. *J. Phys. Chem.* **1990**, *94*, 1050. (b) Marcus, R. A. *J. Phys. Chem.* **1990**, *94*, 4152; addendum, *J. Phys. Chem.* **1990**, *94*, 7742. (c) Marcus, R. A. *J. Phys. Chem.* **1991**, *95*, 2010; addendum, *J. Phys. Chem.* **1995**, *99*, 5742.

(10) Girault, H. H. *J. Electroanal. Chem.* **1995**, *388*, 93.

(11) Smith, B. B.; Halley, J. W.; Nozik, A. J. Submitted.

(12) (a) Senda, M. *Anal. Sci.* **1994**, *10*, 649. (b) Senda, M. *Electrochim. Acta* **1995**, *40*, 2993. (c) Katano, H.; Maeda, K.; Senda, M. *J. Electroanal. Chem.* **1995**, *396*, 391.

(13) For review of the electrochemistry of ITIES see: (a) Girault, H. H.; Schiffrin, D. J. In *Electroanalytical Chemistry*; Bard, A. J., Ed.; Marcel Dekker: New York, 1989; Vol. 15, p 1. (b) Senda, M.; Kakiuchi, T.; Osakai, T. *Electrochim. Acta* **1991**, *36*, 253. (c) Girault, H. H. In *Modern Aspects of Electrochemistry*; Bockris, J. O'M., Conway, B. E., White, R. E., Eds.; Plenum Press: New York, 1993; Vol. 25, p 1.

(14) (a) Geblewicz, G.; Schiffrin, D. J. *J. Electroanal. Chem.* **1988**, *244*, 27. (b) Cunnane, V. J.; Schiffrin, D. J.; Beltran, C.; Geblewicz, G.; Solomon, T. *J. Electroanal. Chem.* **1988**, *247*, 203. (c) Cheng, Y.; Schiffrin, D. J. *J. Electroanal. Chem.* **1991**, *314*, 153.

(15) Nicholson, R. S. *Anal. Chem.* **1965**, *37*, 1351.

(16) Samec, Z.; Marecek, V.; Weber, J.; Homolka, D. *J. Electroanal. Chem.* **1981**, *126*, 105.

(17) Cheng, Y.; Schiffrin, D. J. *J. Chem. Soc., Faraday Trans.* **1993**, *89*, 199.

(18) Wei, C.; Bard, A. J.; Mirkin, M. V. *J. Phys. Chem.* **1995**, *99*, 16033.

(19) Kotov, N. A.; Zaniquelli, M. E. D.; Meldrum, F. C.; Fendler, J. H. *Langmuir* **1993**, *9*, 3710.

(20) Lee, S.; Sung, H.; Han, S.; Paik, W. *J. Phys. Chem.* **1994**, *98*, 1250.

(21) Melroy, O. R.; Buck, R. P. *J. Electroanal.Chem.* **1983**, *151*, 1, and references therein.

(22) Messmer, M. C.; Conboy, J. C.; Richmond, G. L. *J. Am. Chem. Soc.* **1995**, *117*, 8039.

(23) Krause, R. A.; Violette, C. *Inorg. Chim. Acta* **1986**, *113*, 161.

(24) Bard, A. J.; Fan, F.-R. F.; Kwak, J.; Lev, O. *Anal. Chem.* **1989**, *61*, 1794.

(25) Wipf, D. O.; Bard, A. J. *J. Electrochem. Soc.* **1991**, *138*, 489.

(26) Kakiuchi, T.; Senda, M. *Bull. Chem. Soc. Jpn.* **1983**, *56*, 2912.

(27) Unwin, P. R.; Bard, A. J. *J. Phys. Chem.* **1992**, *96*, 5035.

(28) (a) Macpherson, J. V.; Unwin, P. R. *J. Phys. Chem.* **1994**, *98*, 1704. (b) Macpherson, J. V.; Unwin, P. R. *J. Phys. Chem.* **1994**, *98*, 11764. (c) Macpherson, J. V.; Unwin, P. R. *J. Phys. Chem.* **1995**, *99*, 3338.

(29) Kovaleski, J. M.; Wirth, M. *J. Phys. Chem.* **1995**, *99*, 4091.

(30) Solomon, T.; Bard, A. J. *J. Phys. Chem.* **1995**, *99*, 17487.

JP9612700